

UC San Diego

UC San Diego Previously Published Works

Title

Thermal Conductivity of Granular Soil Mixtures with Contrasting Particle Shapes

Permalink

<https://escholarship.org/uc/item/80p0f75z>

Journal

Journal of Geotechnical and Geoenvironmental Engineering, 146(5)

ISSN

1090-0241

Authors

Xiao, Yang
Ma, Guoliang
Nan, Bowen
[et al.](#)

Publication Date

2020-05-01

DOI

10.1061/(asce)gt.1943-5606.0002243

Peer reviewed

1 **Technical Note**

2 **Thermal Conductivity of Granular Soils with Contrasting Particle Shapes**

3 Yang Xiao, M.ASCE¹; Guoliang Ma²; Bowen Nan³; John S. McCartney, F.ASCE³

4 **Abstract:** Particle shape is known to affect the mechanical behavior of sands as it influences packing
5 density and particle contacts. Even though the thermal conductivity of sands also depends on packing
6 density and particle contacts, the effects of particle shape on thermal conductivity are not well
7 understood. A series of thermal needle tests were conducted on five granular soil mixtures with
8 different proportions of rounded and angular glass particles having the same mineral composition
9 and gradation. The maximum and minimum void ratios and the packing density of these mixtures
10 were found to depend on the overall regularity, defined as the average value of the particle's aspect
11 ratio, convexity and sphericity. For a given overall regularity, the thermal conductivity increases with
12 decreasing void ratio or increasing relative density. Interestingly, the overall regularity has a small
13 effect on the thermal conductivity at a given void ratio but has a significant effect on the thermal
14 conductivity at a given relative density. A particle shape-dependent empirical equation is proposed
15 to quantify the effects of relative density and overall regularity on the thermal conductivity of the
16 tested sand.

17 **Keywords:** thermal conductivity; particle shape; overall regularity; relative density; void ratio

18 ¹Professor, State Key Laboratory of Coal Mine Disaster Dynamics and Control; Key Laboratory of New Technology for
19 Construction of Cities in Mountain Area; School of Civil Engineering, Chongqing University, Chongqing, 400045, China.
20 hhuxyanson@163.com.

21 ²Ph.D. Candidate, School of Civil Engineering, Chongqing University, Chongqing, 400045, China. magl09@163.com.

22 ³Master, School of Civil Engineering, Chongqing University, Chongqing, 400045, China. nan_bo_wen@163.com.

23 ⁴Professor and Department Chair, Department of Structural Engineering, University of California San Diego. 9500
24 Gilman Dr., La Jolla, CA 92093-0085. mccartney@ucsd.edu.

25 **Introduction**

26 Particle shape has well-known effects on the characteristics of granular soils including packing
27 density (Cho et al. 2006; Shin and Santamarina 2013; Zheng and Hryciw 2016) and fabric (Maeda et
28 al. 2010; Turner et al. 2016; Zhao and Zhou 2017), and also can have significant effects on
29 mechanical properties like compressibility (Rousé et al. 2008; Shin and Santamarina 2013; Gong and
30 Liu 2017), shear modulus (Cho et al. 2006; Shin and Santamarina 2013), shear strength (Varadarajan
31 et al. 2003; Guo and Su 2007; Rousé et al. 2008; Yang and Wei 2012; Shin and Santamarina 2013;
32 Yang and Luo 2015; Xiao et al. 2019), dilation (Guo and Su 2007; Yang and Luo 2015; Xiao et al.
33 2019), susceptibility to liquefaction (Tsomokos and Georgiannou 2010; Yang and Wei 2012; Yang
34 and Luo 2015), particle breakage during shearing (Afshar et al. 2017; Cavarretta et al. 2017), and
35 failure mode during shearing (Alshibli et al. 2017). Particle shape may also affect the hydraulic
36 conductivity of granular soils (Côté et al. 2011).

37 Although it would be logical that particle shape has an effect on the thermal conductivity,
38 conflicting trends have been noted in the limited studies performed on this topic (Côté and Konrad
39 2005; Yun and Santamarina 2008; Gan et al. 2017; Lee et al. 2017; Fei et al. 2019). Accordingly, the
40 main purpose of this study is to perform thermal needle tests on mixtures of angular and rounded
41 glass particles having different particle shapes under a range of relative densities. The advantage of
42 using glass particles is that they possess the same mineral composition, particle size, particle surface,
43 and gradation, permitting the effect of contrasting particle shape to be isolated. The particle shape is
44 quantified in this study using the overall regularity, defined as the average value of the particle's

45 aspect ratio, convexity and sphericity. Empirical relationships are developed between the thermal
46 conductivity, overall regularity, and relative density for the glass particles tested in this study that
47 may give insight into the importance of particle shape on the thermal properties of granular materials
48 in general.

49 **Materials and Methods**

50 *Materials*

51 Two kinds of glass particles having rounded and angular shapes are used in this study, both of
52 which were obtained from the Hong Kong Siu Tung Glass & Plastic Group Co., Ltd. The average
53 specific gravity for both kinds of particles is 2.35. They have similar uniform gradations with grain
54 sizes ranging from 0.6 to 0.8 mm and can be classified as poorly graded sands according to the unified
55 soil classification scheme (ASTM 2006). The two kinds of glass particles were combined to form
56 five mixtures with different proportions by weight (Figs. 1(a)-1(e)). The designators for the mixtures
57 are A0R100, A25R75, A50R50, A75R25 and A100R0, for example, A25R75 designates 25% angular
58 particles plus 75% rounded particles by weight.

59 *Thermal Conductivity Measurement*

60 Before preparation of the specimens, the maximum and minimum void ratios of each of the
61 mixtures were determined (ASTM 2016a, b) and the results are summarized in Table 1. The
62 specimens were prepared using the undercompaction method proposed by Ladd (1978) to achieve
63 relative densities of 0.3, 0.5, 0.6, 0.7 and 0.8 in a specially-designed mold having a diameter of 50
64 mm and a height of 137 mm. Thermal conductivity was measured using a vertically-oriented thermal

65 needle probe (single needle model TR-1 from Decagon Devices, Pullman, WA) along with a KD2
66 Pro thermal properties analyzer. The TR-1 probe was inserted vertically from the center of the surface
67 of the specimen after preparation. The thermal conductivity of all these specimens was measured five
68 times at room temperature (25 °C) with their average values listed in **Table 2**. More details on thermal
69 needle testing of granular materials can be found in [Xiao et al. \(2018\)](#).

70 **Definition of Particle Shape**

71 Particle shape can be characterized by three parameters, the aspect ratio (A_R), convexity (C_X),
72 and sphericity (S_C) ([Yang and Luo 2015](#); [Xiao et al. 2019](#)). These parameters were determined from
73 binary images of two kinds of glass particles using ImageJ ([Schneider et al. 2012](#)), as shown in **Figs.**
74 **1(f)-1(g)**. These particle shape parameters are defined as

$$75 \quad A_R = D_{\min}^F / D_{\max}^F \quad (1a)$$

$$76 \quad C_X = A / (A + B) \quad (1b)$$

$$77 \quad S_C = P_{eq} / P_r \quad (1c)$$

78 where D_{\min}^F and D_{\max}^F are minimum and maximum Feret diameters, respectively, as shown in **Fig.**
79 **2(a)**; A is the particle area, and $(A + B)$ is the area of particle's convex hull, as defined in **Fig.**
80 **2(b)**; P_{eq} is the perimeter of the equivalent circle which has the same area as the projected area of
81 the particle, and P_r is the perimeter of the projected area of the particle, as shown in **Fig. 2(c)**.

82 [Yang and Luo \(2015\)](#) proposed a particle shape parameter referred to as the overall regularity O_R
83 which can consider the impacts of three particle shape parameters, defined as follows:

$$84 \quad O_R = (A_R + C_X + S_C) / 3 \quad (2)$$

85 The images in **Figs. 2(d)-2(f)** show typical examples of angular particles with specific values of
86 A_R , C_X , S_C and O_R . The particle in **Fig. 2(d)** possesses the largest O_R although its value of C_X
87 is slightly smaller than that of the particle in **Fig. 2(e)**. The particle in **Fig. 2(f)** possesses the smallest
88 A_R , C_X , S_C and O_R .

89 It should be noted that the aspect ratio, convexity, sphericity and overall regularity can only reflect
90 the particle shape of a single particle but not an assembly of particles. Following the studies of (Yang
91 and Luo 2015; Xiao et al. 2019), 500 rounded particles were randomly selected for testing their
92 particle shape parameters and the cumulative distribution curve for each particle shape parameter
93 was obtained for the rounded particle assembly. The particle-shape cumulative distribution curve for
94 the angular particle assembly was obtained in the same way. **Fig. 3** presents the cumulative
95 distribution curves for A_R , C_X , S_C and O_R of two assemblies. The values at 50% of the
96 cumulative distribution are regarded as the representative values for two assemblies according to
97 Yang and Luo (2015) and Xiao et al. (2019). The representative values of particle shape parameters
98 for the mixtures are determined by the combination of the corresponding particle-shape values of the
99 component materials and their percentages by weight (Yang and Luo 2015). For example, the O_R
100 value for A25R75 is determined as follows:

$$\begin{aligned} O_{R_A25R75} &= O_{R_A100R0} \times 25\% + O_{R_A0R100} \times 75\% \\ &= 0.822 \times 25\% + 0.960 \times 75\% = 0.926 \end{aligned} \quad (3)$$

102 The representative values of particle shape parameters for the five mixtures are listed in **Table 1**.
103 Mixtures with higher proportions of rounded particles have larger values of A_R , C_X , S_C and O_R .

104 **Experimental Results and Discussion**

105 ***Effect of Particle Shape on Void Ratio-Relative Density Relationship***

106 The maximum void ratio e_{\max} and minimum void ratio e_{\min} were found to decrease with
 107 increasing overall regularity, as shown in **Fig. 4(a)**. For example, e_{\max} decreases from 0.871 to
 108 0.619, as O_R increases from 0.822 to 0.960. In addition, the difference between e_{\max} and e_{\min}
 109 decreases from 0.204 to 0.058 with an increase in O_R from 0.822 to 0.960. The relationship between
 110 e_{\max} and O_R can be described by a linear regression equation:

111
$$e_{\max} = e_{\max}^0 + \chi_{\max}^e O_R \quad (4)$$

112 where e_{\max}^0 (= 2.308) and χ_{\max}^e (= -1.729) are fitting parameters. Similarly, e_{\min} can be estimated
 113 by

114
$$e_{\min} = e_{\min}^0 + \chi_{\min}^e O_R \quad (5)$$

115 where e_{\min}^0 (= 1.301) and χ_{\min}^e (= -0.792) are fitting parameters. The same trend for e_{\max} and
 116 e_{\min} with respect to particle shape was reported by [Cho et al. \(2006\)](#), [Rousé et al. \(2008\)](#), [Shin and](#)
 117 [Santamarina \(2013\)](#), [Altuhafi et al. \(2016\)](#), [Zheng and Hryciw \(2016\)](#), and [Suh et al. \(2017\)](#).

118 **Figure 4(b)** shows the variations of the measured void ratios with the relative density at different
 119 O_R values. For a given relative density, the void ratio is dependent on the particle shape. For example,
 120 for $I_D=0.5$, the void ratios decrease from 0.769 to 0.590, as O_R increases from 0.822 to 0.960.
 121 Based on **Eqs. (4)** and **(5)**, the relationship between the void ratio and relative density incorporating
 122 the effect of particle shape can be given as

123
$$\begin{aligned} e &= e_{\max} - I_D (e_{\max} - e_{\min}) \\ &= e_{\max}^0 + \chi_{\max}^e O_R - I_D (e_{\max}^0 - e_{\min}^0) - I_D O_R (\chi_{\max}^e - \chi_{\min}^e) \end{aligned} \quad (6)$$

124 As shown in [Fig. 4\(c\)](#), [Eq. \(6\)](#) can reasonably capture the variations of the void ratio with the
125 relative density and overall regularity, according to the maximum error of 0.012 and $R^2=0.989$.

126 *Effect of Particle Shape on Thermal Conductivity-Void Ratio Relationship*

127 [Figure 5\(a\)](#) shows variations of thermal conductivity (λ) with void ratio at different values of
128 O_R . The test data projected on the $\lambda - e$ plane for different O_R values can be fitted by the
129 following empirical relationship:

$$130 \quad \lambda = \lambda_{e0} - \chi_e^\lambda e \quad (7)$$

131 where λ_{e0} (= 0.324) and χ_e^λ (= 0.24) are fitting parameters.

132 The fitting curve obtained from [Eq. \(7\)](#) reasonably describes the variations in thermal
133 conductivity as the data all are encapsulated within a narrow band defined by two lines
134 ($\lambda = (\lambda_{e0} \pm 0.005) - \chi_e^\lambda e$), as shown in [Fig. 5 \(a\)](#). [Fig. 5 \(b\)](#) shows the fitting surface obtained from
135 [Eq. \(7\)](#), which adequately describes the variations in thermal conductivity with void ratio and overall
136 regularity with a maximum absolute error of 0.005 W/m/K.

137 The results in [Fig. 5](#) indicate that the variations in thermal conductivity are mainly affected by the
138 changes in void ratio. At the same void ratio, the influence of the particle shape on thermal
139 conductivity is limited, with an effect of less than 5%. This finding is consistent with the observation
140 from the work by [Yun and Santamarina \(2008\)](#) but inconsistent with the observation by [Côté and](#)
141 [Konrad \(2005\)](#) who reported that the thermal conductivity of angular particles is higher than that of
142 rounded particles at a given void ratio. [Lee et al. \(2017\)](#) reported that the dependence of thermal
143 conductivity on the void ratio for rounded particles is higher than that for angular particles, whereas

144 in the current study the dependence of thermal conductivity on the void ratio is hardly affected by
145 the particle shape. The main reason behind the above differences may be the origin of the data. For
146 example, the data for [Yun and Santamarina \(2008\)](#) include results for six sands tested using the same
147 approach, the data in [Côté and Konrad \(2005\)](#) are from seven published papers, and the data for [Lee
148 et al. \(2017\)](#) include results for nine sands tested using the same approach. However, these three
149 studies ignored some important factors between the sands included in the comparison, such as the
150 particle mineralogy, mean particle size, and particle size distribution which can all affect the thermal
151 conductivity of sands to some extent ([Aduda 1996; Abuel-Naga and Bouazza 2013; Dong et al. 2015;
152 Zhang and Wang 2017; Xiao et al. 2018](#)). In the current study, the mixtures possess the same mineral
153 composition, mean particle size and particle size distribution, so the finding that the effect of the
154 particle shape on thermal conductivity at a given void ratio is more reliable than the conclusions from
155 the other studies. In addition, [Fei et al. \(2019\)](#) found that thermal conductivity increases with
156 increasing particle regularity through an analysis with the finite element method, primarily due to
157 that observation that higher regularity may lead to a higher average coordination number. [Gan et al.
158 \(2017\)](#) use the discrete element method to find that the effective thermal conductivity of granular
159 soils increases with the aspect ratio of ellipsoids. However, it should be noted that the conclusions
160 from [Gan et al. \(2017\)](#) and [Fei et al. \(2019\)](#) are not on the basis of the same void ratio for all mixtures.

161

162 *Effect of Particle Shape on Thermal Conductivity-Relative Density Relationship*

163 It should be noted that it is not possible to obtain the same void ratio for the five mixtures, as
 164 shown in **Fig. 4(b)**, as the maximum void ratio (0.619) of the specimen A0R100 is smaller than the
 165 minimum void ratio (0.667) of the specimen A100R0, as listed in **Table 1**. The relative density, I_D ,
 166 is a common controlling parameter for granular soils, and the same value of I_D is available for each
 167 mixture, as listed in **Table 1**. **Fig. 6(a)** shows variations of the thermal conductivity with the relative
 168 density and overall regularity. The test data projected on the λ - I_D plane for different O_R values
 169 in **Fig. 6(a)** are not in a narrow band, different from the data projected to the λ - e plane in **Fig. 5(a)**.
 170 It is found from the results in **Fig. 6(a)** that an increase in I_D at a given O_R , or an increase in O_R
 171 at a given I_D leads to an increase in λ which is in line with the findings of **Fei et al. (2019)**. For
 172 example, λ increases from 0.154 to 0.172 W/m/K as I_D increases from 0.3 to 0.8 for mixtures
 173 with $O_R=0.891$; or λ increases from 0.149 to 0.189 W/m/K as O_R increases from 0.822 to 0.960
 174 for mixtures with $I_D=0.8$. It is useful to evaluate the thermal conductivity directly from the relative
 175 density at different values of overall regularity. Substituting **Eq. (6)** into **Eq. (7)** gives a relationship
 176 between the thermal conductivity and relative density by incorporating the effect of particle shape,
 177 as follows:

$$178 \quad \lambda = \lambda_{e0} - \chi_e (e_{\max}^0 + \chi_{\max}^e O_R) + \chi_e I_D (e_{\max}^0 - e_{\min}^0) + \chi_e I_D O_R (\chi_{\max}^e - \chi_{\min}^e) \quad (8)$$

179 **Fig. 6(b)** shows that **Eq. (8)** can describe variations of thermal conductivity with the relative
 180 density and overall regularity with $R^2=0.97$ and a maximum absolute error of 0.006 W/m/K.

181 Conclusions

182 The effect of particle shape on thermal conductivity is investigated through a series of thermal

183 needle tests on five mixtures that contain different proportions of rounded and angular particles. The
184 main conclusions are summarized as follows:

185 (1) The overall regularity was used to quantify the particle shape and determine the effect of this
186 variable on thermal conductivity. Both the maximum and minimum void ratios of these mixtures
187 decreased with increasing overall regularity. An equation incorporating the overall regularity in
188 the relationship between the void ratio and relative density was proposed for these mixtures.

189 (2) The thermal conductivity of these mixtures with the same mineral composition and grading
190 increased with decreasing void ratio. However, the thermal conductivity for a given void ratio
191 was less affected by the particle shape. The relationship between the thermal conductivity and
192 void ratio was the same for these mixtures.

193 (3) The thermal conductivity of these mixtures increased with increasing relative density at a given
194 overall regularity or with increasing overall regularity at a given relative density, which implies
195 that the thermal conductivity at a given relative density increased as the proportion of rounded
196 particle increased. An empirical equation incorporating the overall regularity was proposed to
197 estimate the variation of the thermal conductivity with the relative density for these mixtures.

198 **Data Availability**

199 All data and models generated and used during the study appear in the submitted article.

200 **Acknowledgments**

201 The authors would like to acknowledge the financial support from the 111 Project (Grant No.
202 B13024), the National Science Foundation of China (Grant No. 41831282, Grant No. 51678094 and

203 Grant No. 51578096), and the China Postdoctoral Science Foundation (Grant No. 2017T100681).

204 **References:**

205 Abuel-Naga, H. M., and Bouazza, A. (2013). "Thermomechanical behavior of saturated geosynthetic
206 clay liners." *J. Geotech. Geoenviron. Eng.*, 139(4), 539-547.

207 Aduda, B. O. (1996). "Effective thermal conductivity of loose particulate systems." *J. Mater. Sci.*,
208 31(24), 6441-6448.

209 Afshar, T., Disfani, M. M., Arulrajah, A., Narsilio, G. A., and Emam, S. (2017). "Impact of particle
210 shape on breakage of recycled construction and demolition aggregates." *Powder Technol.*,
211 308, 1-12.

212 Alshibli, K. A., Jarrar, M. F., Druckrey, A. M., and Al-Raoush, R. I. (2017). "Influence of Particle
213 Morphology on 3D Kinematic Behavior and Strain Localization of Sheared Sand." *J. Geotech.*
214 *Geoenviron. Eng.*, 143(2).

215 Altuhafi, F. N., Coop, M. R., and Georgiannou, V. N. (2016). "Effect of particle shape on the
216 mechanical behavior of natural sands." *J. Geotech. Geoenviron. Eng.*, 142(12), 04016071.

217 ASTM (2006). "Standard practice for classification of soils for engineering purposes (Unified Soil
218 Classification System)." *D2487-06*, West Conshohocken, PA.

219 ASTM (2016a). "Standard test methods for maximum index density and unit weight of soils using a
220 vibratory table." *D4253-16*, West Conshohocken, PA.

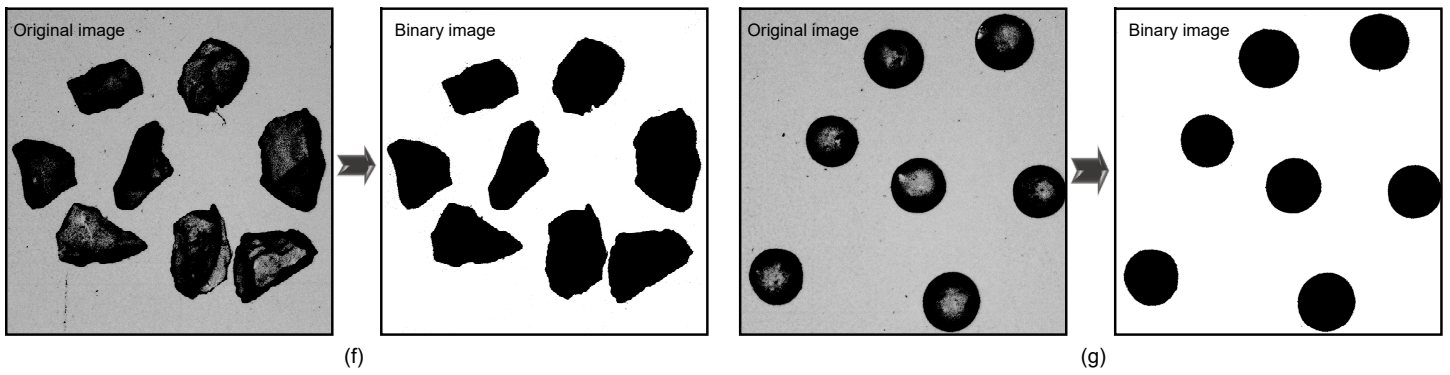
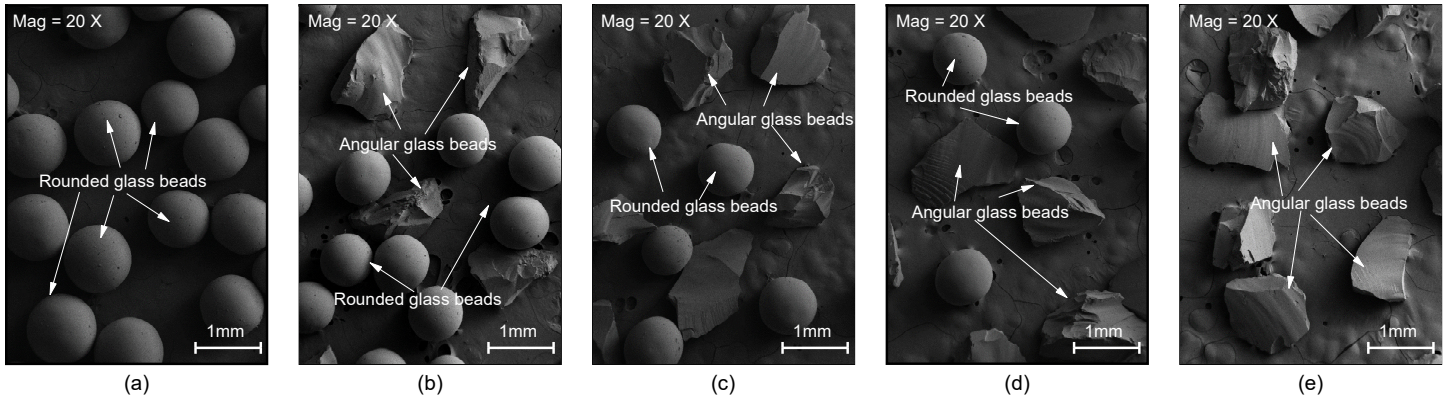
221 ASTM (2016b). "Standard test methods for minimum index density and unit weight of soils and
222 calculation of relative density." *D4254-16*, West Conshohocken, PA.

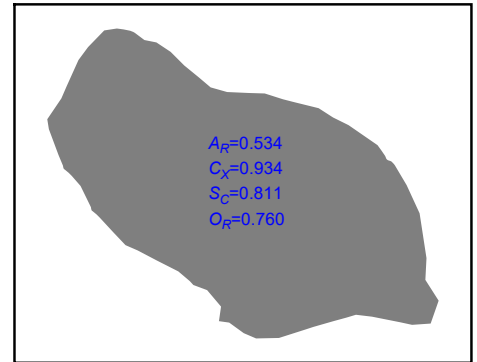
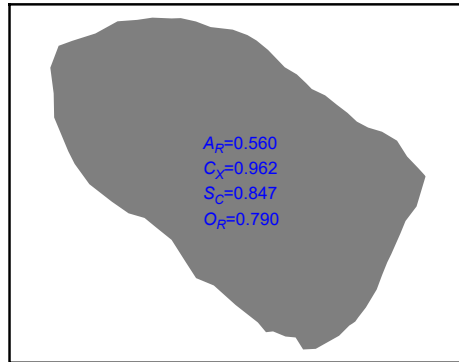
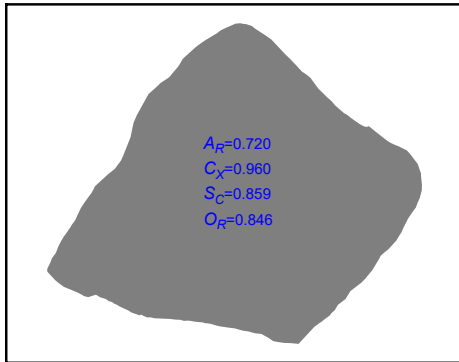
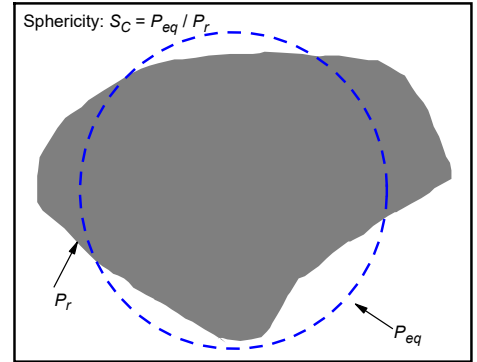
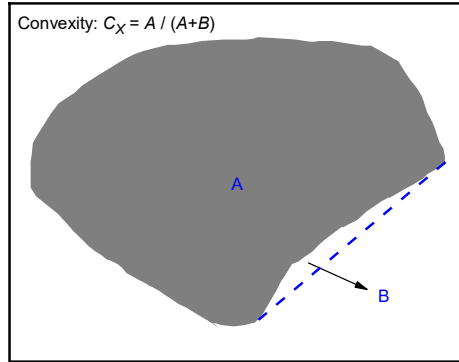
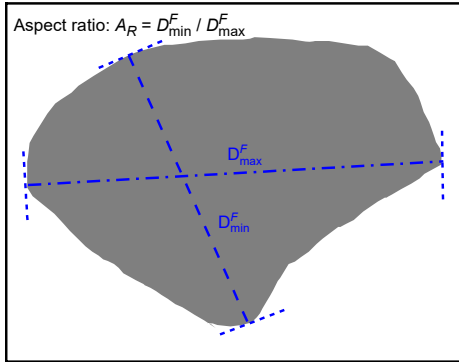
- 223 Cavarretta, I., O'Sullivan, C., and Coop, M. R. (2017). "The relevance of roundness to the crushing
224 strength of granular materials." *Geotechnique*, 67(4), 301-312.
- 225 Cho, G.-C., Dodds, J., and Santamarina, J. C. (2006). "Particle shape effects on packing density,
226 stiffness, and strength: Natural and crushed sands." *J. Geotech. Geoenviron. Eng.*, 132(5),
227 591-602.
- 228 Côté, J., Fillion, M. H., and Konrad, J. M. (2011). "Estimating Hydraulic and Thermal Conductivities
229 of Crushed Granite Using Porosity and Equivalent Particle Size." *J. Geotech. Geoenviron.*
230 *Eng.*, 137(9), 834-842.
- 231 Côté, J., and Konrad, J. M. (2005). "A generalized thermal conductivity model for soils and
232 construction materials." *Can. Geotech. J.*, 42(2), 443-458.
- 233 Dong, Y., McCartney, J. S., and Lu, N. (2015). "Critical review of thermal conductivity models for
234 unsaturated Soils." *Geotech. Geol. Eng.*, 33(2), 207-221.
- 235 Fei, W., Narsilio, G. A., and Disfani, M. M. (2019). "Impact of three-dimensional sphericity and
236 roundness on heat transfer in granular materials." *Powder Technol.*, 355, 770-781.
- 237 Gan, J., Zhou, Z., and Yu, A. (2017). "Effect of particle shape and size on effective thermal
238 conductivity of packed beds." *Powder Technol.*, 311, 157-166.
- 239 Gong, J., and Liu, J. (2017). "Effect of aspect ratio on triaxial compression of multi-sphere ellipsoid
240 assemblies simulated using a discrete element method." *Particuology*, 32, 49-62.
- 241 Guo, P., and Su, X. (2007). "Shear strength, interparticle locking, and dilatancy of granular
242 materials." *Can. Geotech. J.*, 44(5), 579-591.

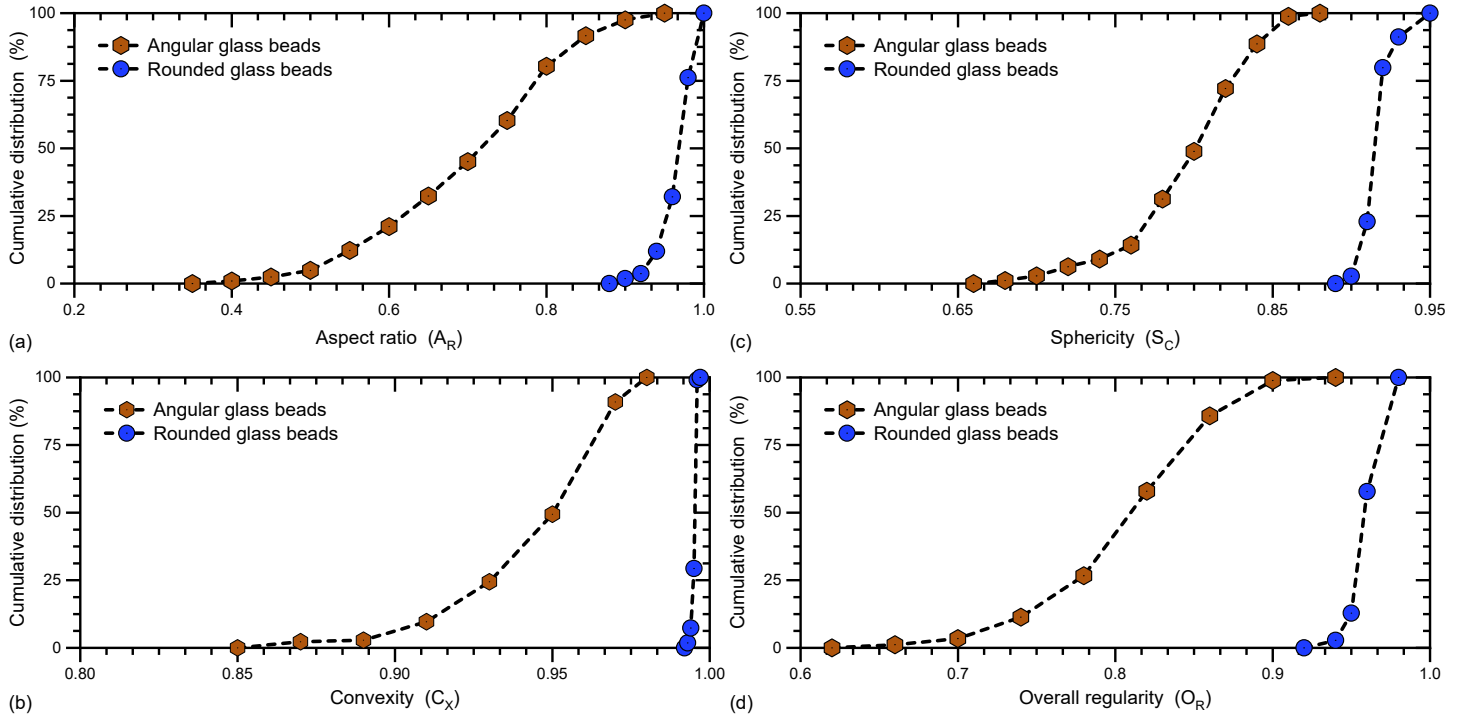
- 243 Ladd, R. S. (1978). "Preparing test specimens using undercompaction." *Geotech. Test. J.*, 1(1), 16-
244 23.
- 245 Lee, C., Suh, H. S., Yoon, B., and Yun, T. S. (2017). "Particle shape effect on thermal conductivity
246 and shear wave velocity in sands." *Acta Geotechnica*, 12(3), 615-625.
- 247 Maeda, K., Sakai, H., Kondo, A., Yamaguchi, T., Fukuma, M., and Nukudani, E. (2010). "Stress-
248 chain based micromechanics of sand with grain shape effect." *Granul. Matter*, 12(5), 499-
249 505.
- 250 Rousé, P. C., Fannin, R. J., and Shuttle, D. A. (2008). "Influence of roundness on the void ratio and
251 strength of uniform sand." *Geotechnique*, 58(3), 227-231.
- 252 Schneider, C. A., Rasband, W. S., and Eliceiri, K. W. (2012). "NIH Image to ImageJ: 25 years of
253 image analysis." *Nat. Methods*, 9(7), 671-675.
- 254 Shin, H., and Santamarina, J. C. (2013). "Role of particle angularity on the mechanical behavior of
255 granular mixtures." *J. Geotech. Geoenviron. Eng.*, 139(2), 353-355.
- 256 Suh, H. S., Kim, K. Y., Lee, J., and Yun, T. S. (2017). "Quantification of bulk form and angularity of
257 particle with correlation of shear strength and packing density in sands." *Eng. Geol.*, 220,
258 256-265.
- 259 Tsomokos, A., and Georgiannou, V. N. (2010). "Effect of grain shape and angularity on the undrained
260 response of fine sands." *Can. Geotech. J.*, 47(5), 539-551.
- 261 Turner, A. K., Kim, F. H., Penumadu, D., and Herbold, E. B. (2016). "Meso-scale framework for
262 modeling granular material using computed tomography." *Comput. Geotech.*, 76, 140-146.

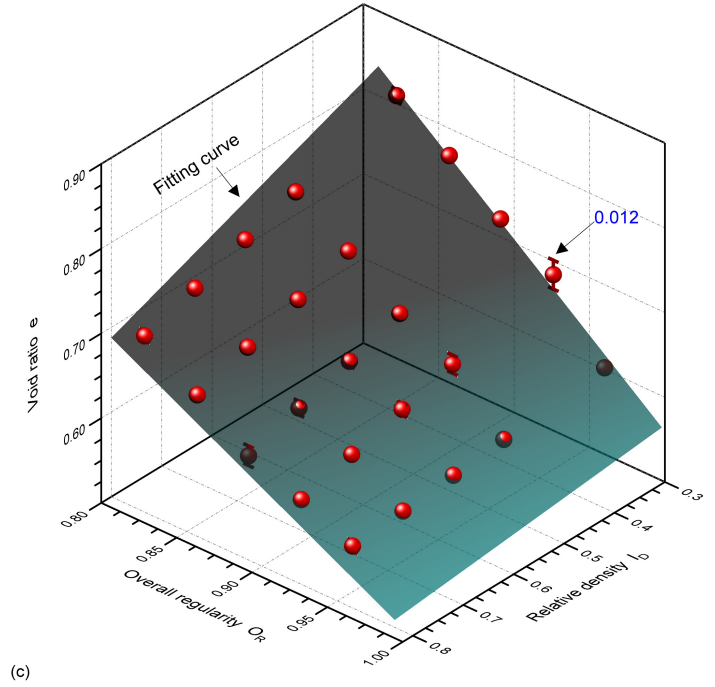
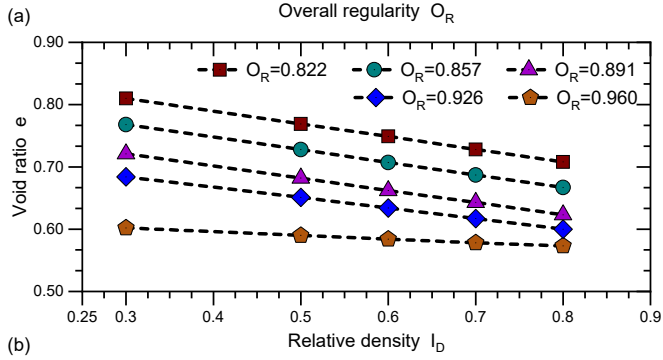
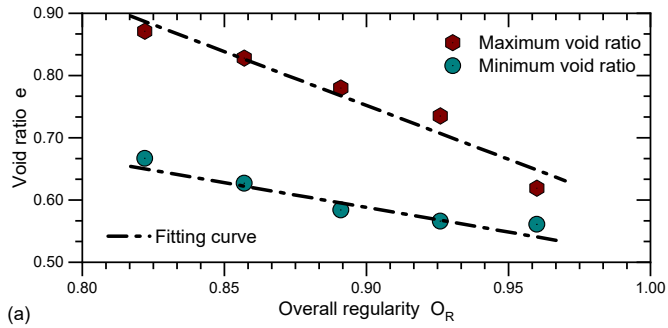
- 263 Varadarajan, A., Sharma, K. G., Venkatachalam, K., and Gupta, a. K. (2003). "Testing and Modeling
264 Two Rockfill Materials." *J. Geotech. Geoenviron. Eng.*, 129(3), 206-206.
- 265 Xiao, Y., Liu, H. L., Nan, B. W., and McCartney, J. S. (2018). "Gradation-dependent thermal
266 conductivity of sands." *J. Geotech. Geoenviron. Eng.*, 144(9), 06018010.
- 267 Xiao, Y., Long, L., Evans, T. M., Zhou, H., Liu, H., and Stuedlein, A. W. (2019). "Effect of Particle
268 Shape on Stress-Dilatancy Responses of Medium-Dense Sands." *J. Geotech. Geoenviron.
269 Eng.*, 145(2), 04018105.
- 270 Yang, J., and Luo, X. D. (2015). "Exploring the relationship between critical state and particle shape
271 for granular materials." *J. Mech. Phys. Solids*, 84, 196-213.
- 272 Yang, J., and Wei, L. M. (2012). "Collapse of loose sand with the addition of fines: the role of particle
273 shape." *Geotechnique*, 62(12), 1111-1125.
- 274 Yun, T. S., and Santamarina, J. C. (2008). "Fundamental study of thermal conduction in dry soils."
275 *Granul. Matter*, 10, 197-207.
- 276 Zhang, N., and Wang, Z. (2017). "Review of soil thermal conductivity and predictive models." *Int. J.
277 Therm. Sci.*, 117, 172-183.
- 278 Zhao, S., and Zhou, X. (2017). "Effects of particle asphericity on the macro- and micro-mechanical
279 behaviors of granular assemblies." *Granul. Matter*, 19(2), 38.
- 280 Zheng, J., and Hryciw, R. D. (2016). "Index void ratios of sands from their intrinsic properties." *J.
281 Geotech. Geoenviron. Eng.*, 142(12), 06016019.

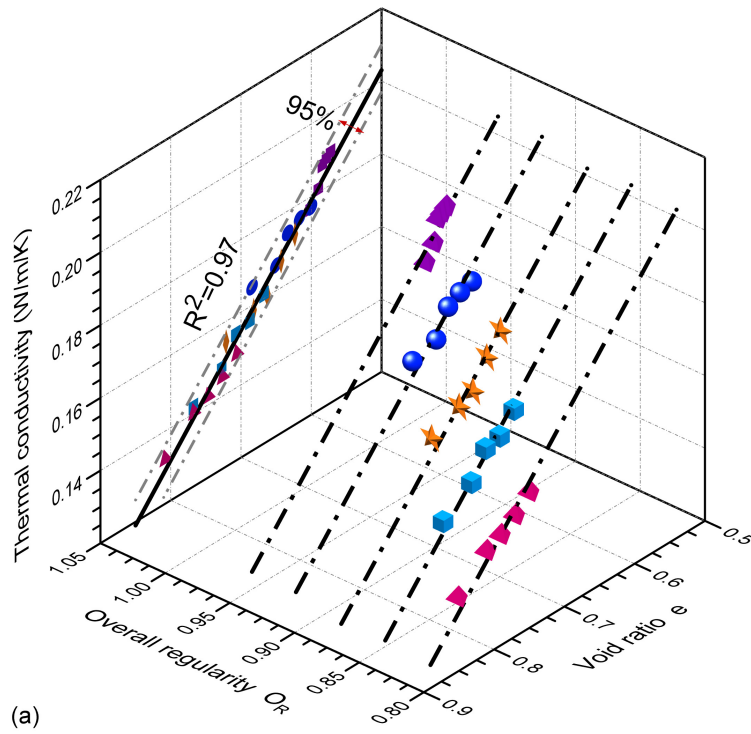
282



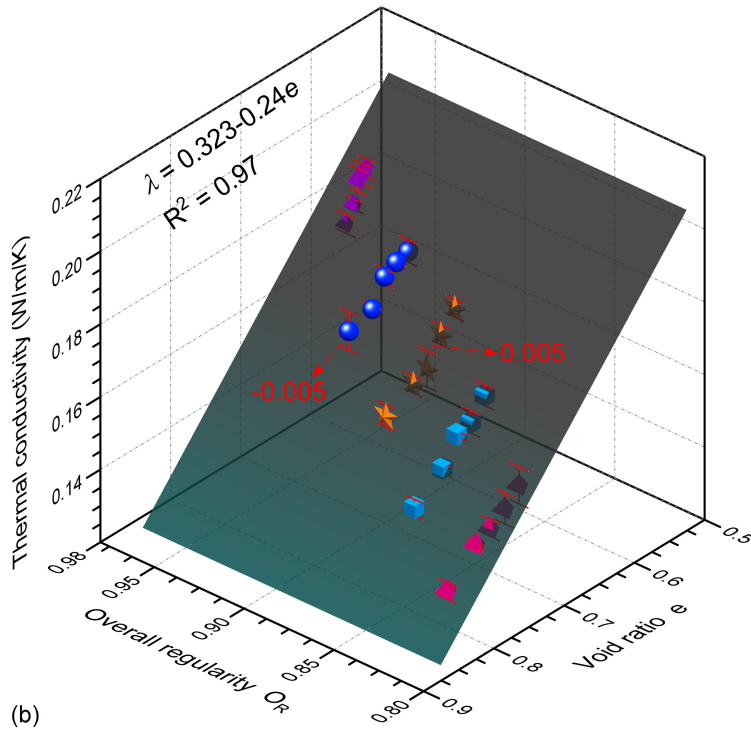








(a)



(b)

